Probing long-lived plasmonic-generated charges in TiO_2 / Au by high resolution x-ray absorption spectroscopy

Lucia Amidani,[a],[b]* Alberto Naldoni,[c]* Marco Malvestuto,[d] Marcello Marelli,[c] Pieter Glatzel,[b] Vladimiro Dal Santo,[c] and Federico Boscherini[a]

Abstract: Exploiting plasmonic Au nanoparticles to sensitize TiO_2 to visible light is a widely employed route to produce efficient photocatalysts. However, a description of the atomic and electronic structure of the semiconductor sites in which charges are injected, of great importance to understand the underlying physical mechanisms and to improve the design of catalysts with enhanced photoactivity, is still not available. We investigated changes in Ti local electronic structure of pure and N-doped nanostructured TiO_2 loaded with Au nanoparticles during continuous selective excitation of the Au localized surface plasmon resonance with X-ray Absorption Spectroscopy (XAS) and Resonant Inelastic X-ray Scattering (RIXS). Spectral variations strongly support the presence of long-lived charges localized on Ti ~~3d states~~ atoms at the semiconductor surface, giving rise to new laser-induced low-coordinated Ti sites.

The search for innovative and efficient schemes for the use of solar energy is motivated by the increasing demand for clean energy. Materials used in artificial photosynthesis, e.g. in water splitting/CO_2 reduction,[1,2] also find application in important chemical processes such as wastewater treatment, pollutant removal, and production of fine chemicals.[3,4]

Wide bandgap semiconductors, i.e. TiO_2, have low conversion efficiency due to their poor absorption of solar light. Among the new concepts introduced to increase light harvesting, the use of plasmonics is particularly promising.[3] Plasmonic metal nanoparticles (NPs), indeed, have extremely high absorption cross-sections ~~at~~ in correspondence of the Localized Surface Plasmon Resonance (LSPR) wavelength, which is easily tailored across the solar spectrum acting on NPs shape and size. Upon illumination of LSPR band, plasmonic NPs can sensitize semiconductors to below bandgap light and create charge-separated states with prolonged lifetime.[4] The main interaction mechanism leading to sensitization is the generation of "hot electrons (e^-)" having sufficient energy to overcome the Schottky barrier at the metal/TiO_2 interface and be injected into the TiO_2 conduction band (CB). In parallel, the unique ability of plasmonic NPs to concentrate electromagnetic fields in nanoscale volumes can induce a secondary process where plasmon oscillation resonate with the semiconductor band gap, i.e. plasmonic resonant energy transfer (PRET).[4] Recently, plasmonic driven processes (whether charge or energy transfer) have been the focus of intense research.[3,4] For example, Mubeen *et al.* reported an efficient, water splitting device based on Au nanorods array/TiO_2 where all charge carriers involved in the reaction steps were hot e^- excited by Au LSPR excitation.[2] Tailored composite materials and bimetallic plasmonic NPs have also shown high efficiency in driving extensive number of selective chemical reactions.[3,4]

When used to convert solar light into chemical energy, metal oxides undergo small changes in the electronic and structural properties that drive the catalytic process. Photogenerated charges can in fact induce transient modifications like variation of metal oxidation state and/or the local reconstruction of catalytic sites. Pump-probe, time resolved and *in-operando* x-ray spectroscopies[5] can detect such modifications by probing the local electronic and structural properties of a selected atomic species and shed light on key steps of the catalytic process, a fundamental achievement to design efficient and cheap photocatalysts.

Figure 1. (a) HRTEM images showing the sharp interface formed after Au NPs deposition on TiO_2 samples. (b) Scheme of the experimental set-up.

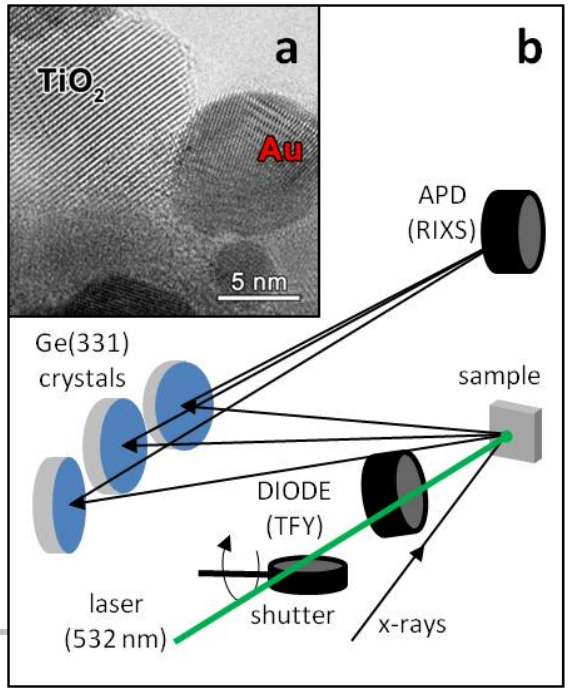

[a] Dr. L. Amidani and Prof. F. Boscherini
Department of Physics and Astronomy
University of Bologna
Viale Berti-Pichat 6/2, 40127 Bologna, Italy
E-mail: lucia.amidani3@unibo.it;
[b] Dr. L. Amidani and Dr. Pieter Glatzel
ESRF - The European Synchrotron
71 Avenue des Martyres, Grenoble 38000 , France
E-mail: lucia.amidani@esrf.fr
[c] Dr. A. Naldoni, Dr. M. Marelli, Dr. V. Dal Santo
CNR-ISTM
Via Golgi 19, 20133 Milano, Italy
E-mail: a.naldoni@istm.cnr.it
[d] Dr. M. Malvestuto
Elettra-Sincrotrone Trieste
S.S. 14 Km 163.5 Area Science Park Trieste, I-34149, Italy

Supporting information for this article is available on the WWW under http://…

Despite the fact that many approaches that couple plasmonic NPs to semiconductors have been reported so far, the details on structure and electronic nature of trapping sites are still unknown. Tracing the modifications that LSPR excited carriers induce on the density of states of the metal oxide can potentially provide atomistic description of charge localization sites giving important details to improve catalysts design.

Long lifetimes, in the order of μs to ms, and proximity to the surface are essential requirements for photogenerated carriers to efficiently participate to chemical reactions. Light induced variations in atomic and electronic structure due the presence of long-lived charges can be detected by acquiring spectra during continuous Au LSPR excitation. A spectrum acquired under this condition will be the average of characteristic lineshapes of all intermediate states, each weighted by the lifetime. Spectral variations relative to long-lived charges are then amplified with respect to carriers that rapidly recombine.

Herein we report a XANES/RIXS investigation of TiO_2/Au powders during laser excitation of Au NPs LSPR. The spectral variations observed were significant and strongly support a laser-induced reduction of a small percentage of Ti atoms due to long-lived hot electrons that remain trapped in Ti sites at the semiconductor surface after being injected from the Au NPs.

We measured powders of pure and N-doped TiO_2 (anatase) of 15 nm average size loaded with 10 wt. % Au NPs of 5 nm mean diameter. Both UV-vis absorption spectra (Figure S1) show the Au LSPR band centered at about 550 nm. However, the absorption of N-TiO_2 extends to the visible spectrum reflecting its reduced band gap and yellow color. In Figure 1a a representative HRTEM image of TiO_2/Au shows the sharp interface between TiO_2 and Au NPs, a crucial morphological feature to assure an efficient Au – TiO_2 interaction.

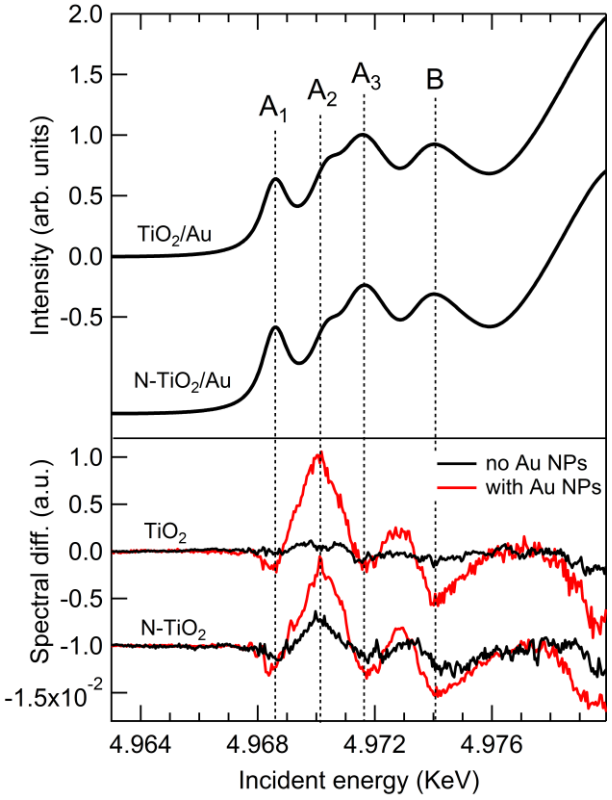

Figure 2. The upper panel shows the pre-edge region of TiO_2/Au and N-TiO_2/Au measured in TFY obtained by averaging fifty laser off scans. The lower panel reports differences between laser on – laser off average spectra acquired on bare powders (black line) and plasmonic TiO_2/Au powders (red line).

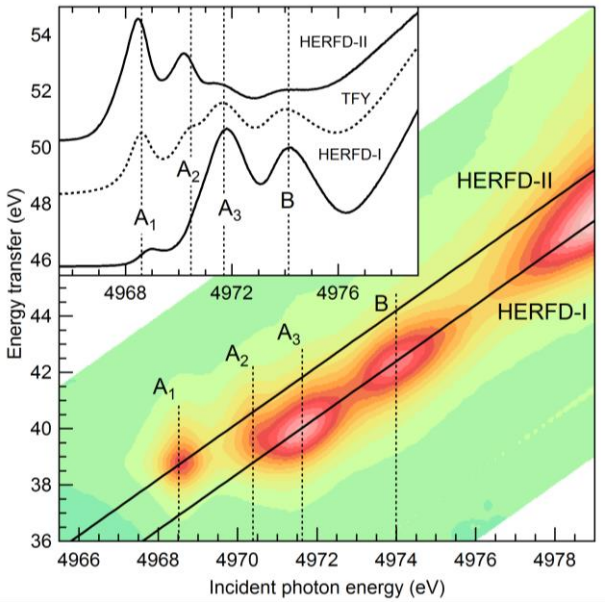

Figure 3. *1s3p* RIXS plane of the pre-edge region of Ti K-edge spectrum for N-TiO_2. *1s3p* RIXS plane is obtained by collecting Ti K_β fluorescence while scanning Ti K-edge with the incident x-ray beam. Incident energies of $A_{1\text{-}3}$ and B transitions are indicated by dotted black lines, while HERFD-I and HERFD-II cuts are shown with solid black lines. The inset shows the pre-edge region of Ti K-edge spectrum for N-TiO_2 measured in TFY, HERFD-I and HERFD-II.

The experiment was performed on the ID26 beamline at the ESRF[56] with the set-up shown schematically in Figure 1b. We recorded RIXS, High Energy Resolution Fluorescence Deteced (HERFD) and Total Fluorescence Yield (TFY) XANES (see SI for details). Au NPs were excited with a 532 nm 200 mW continuous wave laser and a shutter was used to alternately record laser on/laser off spectra.

Figure 2 reports laser effects on bare and Au-loaded powders in the pre-edge region measured in TFY. Average of laser off scans, the non-excited spectra, are in the top panel and show the typical lineshape of anatase, with four features labeled $A_{1\text{-}3}$ and B related to Ti 3d states.[67] Laser on/laser off spectral differences are reported in the bottom panel for bare and Au loaded powders. Laser irradiation on bare powders leaves unchanged pure TiO_2 while inducing weak variations in N-TiO_2. As soon as Au NPs are added to oxides, large changes appear in the whole pre-edge region of pure TiO_2 and the ones in N-TiO_2 are strongly enhanced. We recall that N-TiO_2 slightly absorbs 532 nm green light because of the reduced band gap due to N doping. The amplitude and shape of the differential signal is similar for the two powders, hence it can not be related to PRET, which is energetically allowed only in N-TiO_2 and not in pure TiO_2.[4e] The laser induces a strong increase of A_2 (roughly 1.4%) and modulates the whole pre-edge region as seen by the oscillatory behavior of both differential signals. The lineshape of Ti pre-edge might be also affected by T variations.[78] We estimated the T increase expected in our experimental conditions and found it negligible, thus excluding also a contribution from sample heating (see calculation in SI).[89] Therefore, we believe that the variations observed on the

electronic structure of Ti are a consequence of hot e^- injection into the TiO_2 CB.

To understand what causes such variations of Ti local electronic structure, we focused on N-TiO_2 and recorded RIXS data. In Figure 3 we report the RIXS plane in the region of the K_β emission (*1s3p* RIXS) of N-TiO_2 pre-edge, where the four features $A_{1\text{-}3}$ and B appear at different energies: A_3, B and the main edge lie on the RIXS cut named HERFD-I (detection of K_β maximum) while A_1 and A_2 ~~lie on~~ are peaked at lower emitted energies and can be isolated from the rest of the spectrum by acquiring HERFD-II.

The comparison of HERFD-I, HERFD-II and in TFY pre-edges is shown in the inset of Figure 3. As in most transition metal oxides, TiO_2 pre-edge probes metal *d* states, directly through quadrupolar transitions or indirectly through dipole transitions to *d–p* hybridized states.[9,10] Detailed peak assignment has been debated at length due to the complexity of this nominally simple material (TiO_2 has formally empty d band). In general it can be stated that the pre-edge probes Ti t_{2g} and e_g bands, specifically A_1 and A_3 probe mainly the t_{2g} band and A_2 and B the e_g. The separation of pre-edge peaks in ~~two~~ different cuts of the RIXS plane reflects the effect of the core-hole potential, which in turn depends on the localization of the final states reached.[11a] A_1 and A_2 have thus been associated to transitions to states strongly localized on the absorber.[11b-e,9] On the other hand, investigation of nanosized TiO_2 pointed out that A_2 is particularly sensitive to crystallinity[12,14] and NP size[13,2] so that A_2 intensity ~~has~~ can be~~en~~ correlated to low-coordinated Ti sites at the surface.

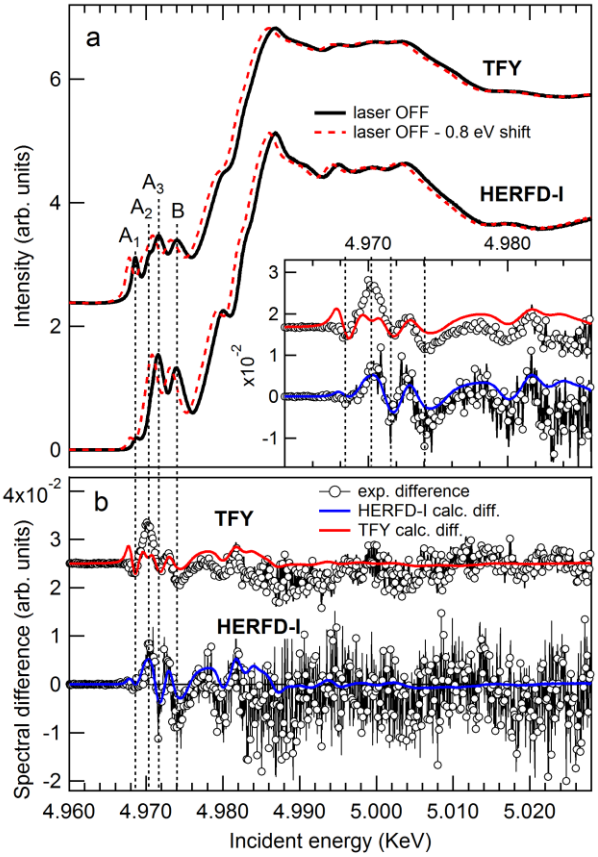

Figure 4. Effect of LSPR excitation in full XANES acquired in TFY and HERFD-I on N-TiO_2/Au. Panel a: experimental (black continuous line) and red-shifted (red dashed line) laser off spectra. Panel b: TFY and HERFD-I laser on – laser off differences of experimental data (black dotted line) and generated shifted – unshifted differences of TFY (red line) and HERFD-I (blue line) spectra. The inset in panel a shows a magnification of the pre-edge region. Vertical dotted lines are added as guide to the eye to mark the position of pre-edge peaks.

We used RIXS to decouple the laser effect on A_1 and A_2 from the rest of the spectrum by acquiring HERFD-I and HERFD-II spectra separately. Results on HERFD-I full XANES are shown in Figure 4 together with TFY acquired in parallel. Figure 4a reports laser off spectra and panel Figure 4b the laser induced spectral differences, which are significant in the pre-edge region while in the post-edge data essentially scatter around zero. Studies of TiO_2/dye composites for solar cell application support e^- injection from the dye to TiO_2 and recent studies have indicated low coordinated Ti sites as most probable e^- traps 100 ps after the injection, implying that a reduction of Ti oxidation state is expected after trapping.[5c]

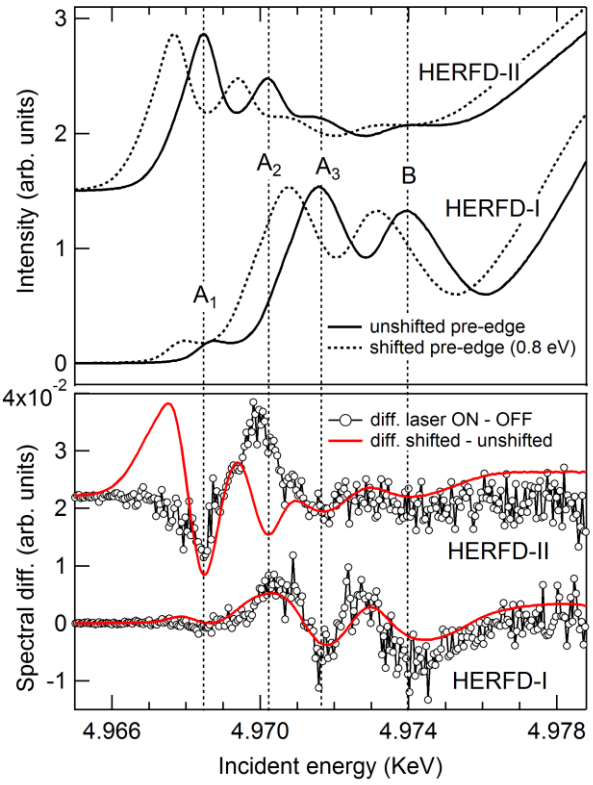

Figure 5. The upper panel shows experimental (continuous line) and red-shifted (dashed line) laser off HERFD-II and HERFD-I pre-edges of N-TiO_2/Au. The bottom panel displays experimental laser on – laser off differences (black line) compared to generated shifted – unshifted differences (red line) for HERFD-II and HERFD-I. HERFD-I laser variations are reproduced fairly well by red-shifting experimental data. On the contrary, HERFD-II laser variations are not compatible with a red-shift of transitions.

To verify if our results are consistent with an edge shift due to Ti reduction, we red-shifted laser off TFY and HERFD-I scans and computed the difference between shifted – unshifted spectra. Generated differences are reported on experimental data in Figure 4b and a magnified view of the pre-edge region is also shown in the inset of Figure 4a. We tested red-shifts from 0 to –2 eV and found best agreement for –0.8 eV. The weight used to best match generated differences with experimental data is 0.74%. The agreement between HERFD-I experimental

data and generated difference is excellent, both shape and amplitude of variations induced by hot e^- transfer are well reproduced over the whole XANES range. The agreement is very good also for TFY XANES, but the mismatch in correspondence of peaks A_1 and A_2 points out the need to separately investigate laser effects on HERFD-II.

The result of a cycle of laser on – laser off scans of HERFD-II are summarized in Figure 5 and compared with HERFD-I results: the top panel reports laser off spectra and their shifted counterpart for N-TiO_2/Au. The bottom panel displays experimental differences between laser on and laser off scans compared with 0.74% generated differences. The experimental results on HERFD-II are clearly not consistent with a red-shift, here Au LSPR – TiO_2 interaction induces rather an increase of A_2 coupled with a slight decrease of A_1.

The red-shift of HERFD-II is consistent with the presence of extra-charge in 3d states the vicinity of a small percentage of Ti atoms, since the main parameter affecting transitions to states with *p* character (edge and dipolar pre-edge peaks) is the change in the valence electron distribution around metal atoms.[14] On the other hand, in HERFD-II the presence of extra charge does not shift A_1 and A_2, whose energy position is determined by the effect of the core-hole potential. However it affects their intensities and the pronounced increase of A_2 points out the increase of recalls the effect on the pre-edge of low-coordinated Ti sites at the surface, characterized by extra-charge due to dangling bonds or structural distortions.[13b-c] . The twofold behavior observed in our data is therefore the signature of long-lived electrons that after injection are remain trapped in 3*d*–*p*[10] states of Ti atoms at the surface and appear as new laser-induced low-coordinated Ti sites. Based on our result, the conversion efficiency of photons absorbed into surface trapped electrons is ~0.1% (see SI for details).

Interactions between molecules and the TiO_2 surface play a key role in photocatalytic processes like water splitting, environmental remediation, and synthesis of fine chemicals. Anatase TiO_2 surface shows both fully coordinated (6c) and low-coordinated (5c) Ti atoms, as well as threefold (3c) and twofold (2c) coordinated oxygens.[15] Defective sites, because of the absence of some chemical bonds, present local extra charge and partial structural rearrangement which favor the adsorption of small molecules in their vicinity if compared to stoichiometric surface regions. In addition, considering metal NPs supported on oxides, the interface clearly plays a critical role providing enhanced reactivity.[16] Similarly, we suggest that in plasmonic TiO_2 / Au, hot e^- remain trapped near the composite interface in Ti 3d-p states and generate sites with a similar electronic and structural nature of the already existing low-coordinated ones therefore acting as additional sites for molecules adsorption and providing photogenerated charges to start the catalytic reaction.

In conclusion, with synchrotron-based XAS and RIXS we provided atomistic insights into the electronic and structural localization of plasmonic generated charges. Our investigation indicates that part of the injected electrons survive longer, being captured at 3d Ti sites concentrated nearby the surface. These trapped charges have all the characteristics required to be the active sites in plasmonic photocatalysis.

Acknowledgements

Financial support from Regione Lombardia through the projects "TIMES: technology and materials for the efficient use of solar energy" − Accordo Quadro Regione Lombardia − CNR and from MIUR through the FIRB projects "Oxides at the nanoscale: multifunctionality and applications" (RBAP115AYN) and "Low cost photoelectrodes architectures based on the redox cascade principles for artificial photosynthesis" (RBFR13XLJ9) and project EX-PRO-REL (Elettra Sincrotrone Trieste) are gratefully aknowledged. We acknowledge: J.-D. Cafun, S. Bauchau and J. Jacobs of the ESRF, Prof. Elena Selli and Francesca Riboni for supplying of N-TiO_2.

Keywords: plasmonic • hot electrons • photocatalysis • trapping • x-ray absorption spectroscopy • resonant inelastic x-ray scattering

[1] a) M. Grätzel, *Nature* **2001**, *414*, 338-344; b) Z. Li, W. Luo, M. Zhang, J. Feng, Z. Zou, *Energy Environ. Sci.* **2013**, *6*, 347-370; c) M. Marelli, A. Naldoni, A. Minguzzi, M. Allieta, T. Virgili, G. Scavia, S. Recchia, R. Psaro, V. Dal Santo, *ACS Appl. Mater. Interfaces.* **2014**, *6*, 11997-12004.

[2] S. Mubeen, J. Lee, N. Singh, S. Kraemer, G. D. Stucky, M. Moskovits, *Nat. Nanotech.* **2013**, *8*, 247-251.

[3] a) S. Linic, P. Christopher, D. B. Ingram, *Nature Materials* **2011**, *10*, 911-921; b) C. Clavero, *Nature Photonics* **2014**, *8*, 95-103; c) S. K. Cushing, J. Li, F. Meng, T. R. Senty, S. Suri, M. Zhi, M. Li, A. D. Bristow, N. Wu, *J. Am. Chem. Soc.* **2012**, *134*, 15033-15041; d) X. Huang, Y. Li, Y. Chen, H. Zhou, X. Duan and Y. Huang, *Angew. Chem. Int. Ed.* **2013**, *52*, 6063-6067; e) Y. Sugano, Y. Shiraishi, D. Tsukamoto, S. Ichikawa, S. Tanaka, T. Hirai, *Angew. Chem. Int. Ed.* **2013**, *52*, 5295-5299.

[4] a) Y. Tian, T. Tatsuma, *Chem. Commun.* **2004**, 1810-1811; b) A. Furube, L. Du, K. Hara, R. Katoh, M. Tachiya, *J. Am. Chem. Soc.* **2007**, *129*, 14852-14853; c) Y. Tian, Tetsu Tatsuma, *J. Am. Chem. Soc.* **2005**, *127*, 7632-7637; d) Y. Nishijima, K Ueno, Y. Yokota, K. Murakoshi, H. Misawa, *J. Phys. Chem. Lett.* **2010**, *1,* 2031-2036; ae) Z. Liu Z, W. Hou, P. Pavaskar, M. Aykol, S.B. Cronin., *Nano Lett.* 2011, *11*, 1111–1116; bf) R. Long, O. V. Prezhdo, *J. Am. Chem. Soc.* **2014**, *136*, 4343-4354; cg) F. Wang, C. Li, H. Chen, R. Jiang, L.-D. Sun, Q. Li, J. Wang, J. C. Yu, C.-H. Yan, *J. Am. Chem. Soc.* **2013**, *135*, 5588-5601; dh) R. Long, K. Mao, M. Gong, S. Zhou, J. Hu, M. Zhi, Y. You, S. Bai, J. Jiang, Q. Zhang, X. Wu and Y. Xiong, *Angew. Chem. Int. Ed.* **2014**, *53*, 3205-3209; ei) J. S. DuChene, B. C. Sweeny, A. C. Johnston-Peck, D. Su, E. A. Stach, W. D. Wei, *Angew. Chem. Int. Ed.* **2014**, *53*, 7887-7891.

[5] a) A. Minguzzi, O. Lugaresi, E. Achilli, C. Locatelli, A. Vertova, P. Ghigna, S. Rondinini, *Chem. Sci.* **2014**, *5*, 3591–3597; b) H. G. Sanchez Casalongue, M. Ling Ng, S. Kaya, D. Friebel, H. Ogasawara, A. Nilsson, *Angew. Chem. Int. Ed.* **2014**, *53*, 7169-7172; c) M. H. Rittmann-Frank, C. J. Milne, J. Rittmann, M. Reinhard, T. J. Penfold, M. Chergui, *Angew. Chem. Int. Ed.* **2014**, *53*, 5858-5862.

[65] C. Gauthier, V. Sole, R. Signorato, J. Goulon, E. Moguiline, *J. Synchrotron Radiat.* **1999**, *6*, 164-166.

[76] L. A. Grunes, *Phys. Rev. B* **1983**, *27*, 2111-2131.

[87] a) O. Durmeyer, E. Beaurepaire, J.-P. Kappler, C. Brouder, F. Baudelet, *J. Phys.: Condens. Matter* **2010**, *22*, 125504-125509; b) C. Brouder, D. Cabaret, A. Juhin and P. Sainctavit, *Phys. Rev. B* **2010**, *81*, 115125-115130.

[98] A. O. Govorov, H. Richardson, *Nonotoday* **2007**, *2*, 30-38.

[109] T. Yamamoto, *X-ray Spectrom.* **2008**, *37*, 572-584.

[110] ad) P. Glatzel, M. Sikora and M. Fernández-García, *Eur. Phys. J. Special Topics* **2009**, *169*, 207-214; ba) Y. Joly, D. Cabaret, H. Renevier and C. R. Natoli, *Phys. Rev. Lett.* **1999**, *82*, 2398-2401; cb) D. Cabaret, A. Bordage, A. Juhin, M. Arfaoui, E. Gaudry, *Phys. Chem. Chem. Phys.* **2010**, *12*, 5619-5633; dc) F. M. F. de Groot, *X-ray Absorption Fine Structure – XAFS13* **2007**, 37-43; e) J. Szlachetko, J. Sá, *Cryst. Eng. Comm.* **2013**, *15*, 2583-2587.

[121] a) T. L. Hanley, V. Luca, I. Pickering and R. F. Howe, *J. Phys. Chem. B* **2002**, *106*, 1153-1160; b) S. J. Stewart, M. Fernández-García, C.

Belver, B. Simon Mun and F. G. Requejo, *J. Phys. Chem. B* **2006**, *110*, 16482-16486.

[132] a) H. Zhang, B. Chen and J. F. Banfield, *Phys. Rev. B* **2008**, *78*, 214106-214117; b) V. Luca, S. Djajanti and R. F. Howe, *J. Phys. Chem. B* **1998**, *102*, 10650-10657; c) V. Luca, *J. Phys. Chem. C* **2009**, *113*, 6367-6380; d) X. Chen, T. Rajh, Z. Wang and M. C. Thurnauer, *J. Phys. Chem. B* **1997**, *101*, 10688-10697.

[13] M. H. Rittmann-Frank, C. J. Milne, J. Rittmann, M. Reinhard, T. J. Penfold, M. Chergui, *Angew. Chem. Int. Ed.* **2014**, *126*, 5968-5972.

[14] A. H de Vries, L. Hozoi, R. Broer, *Int. J. Quantum Chem.* **2003**, *91*, 57-61.

[15] a) A. Tilocca, A. Selloni, *J. Chem. Phys.* **2003**, *119*, 7445-7450; b) E. Finazzi, C. Di Valentin, G. Pacchioni, A. Selloni, *J. Chem. Phys.* **2008**, *129*, 154113; c) B. J. Morgan, G. W. Watson, J. *Phys. Chem. C* **2010**, *114*, 2321; d) A. Janotti, J. B. Varley, P. Rinke, N. Umezawa, G. Kresse, C. G. Van de Walle, *Phys. Rev. B* **2010**, *81*, 085212.

[16] a) T. V. W. Janssensa, B. S. Clausena, B. Hvolbækb, H. Falsigc, C. H. Christensenc, T. Bligaardb, J. K. Nørskov, *Topics in Catal.* **2007**, *44*, 15-26; b) M. Cargnello, V. V. T. Doan-Nguyen, T. R. Gordon, R. E. Diaz, E. A. Stach, R. J. Gorte, P. Fornasiero, C. B. Murray, *Science* **2013**, *331*, 771-773;

The atomistic description of TiO_2 electronic and structural changes due to the injection of hot electrons is reported. Plasmonic charges are trapped on Ti ~~3d states~~ atoms at the semiconductor surface, giving rise to transient low-coordinated Ti sites having sufficient lifetime to play a major role in catalytic processes.

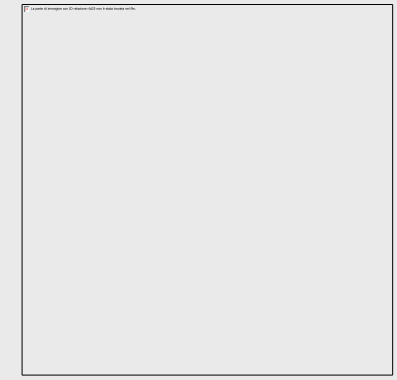

Lucia Amidani, Alberto Naldoni,* Marco Malvestuto, Marcello Marelli, Pieter Glatzel, Vladimiro Dal Santo, and Federico Boscherini*

Page No. – Page No.

Probing long-lived plasmonic-generated charges in TiO_2 / Au by high resolution x-ray absorption spectroscopy